Supplementary Information

Metal cation detection based on a stable n-channel accumulation organic electrochemical transistor

Cheng Shi,[a] Xingyu Jiang,[a] Qi Wang,[a] Xinyu Dong,[a] Chuan Xiang,[a] Zi Wang,[b] Lifeng Chi*[ac] and Lizhen Huang*[a]

[a] Institute of Functional Nano & Soft Materials (FUNSOM), Soochow University, 199 Ren'ai Road, Suzhou, 215123, Jiangsu, P. R. China

[b] Suzhou Laboratory, 388 Ruoshui Road, Suzhou 215123, P. R. China

[c] Macao Institute of Materials Science and Engineering (MIMSE), MUST-SUDA Joint Research Center for Advanced Functional Materials, Macau University of Science and Technology, Taipa 999078, Macao, China

Supplementary Figures

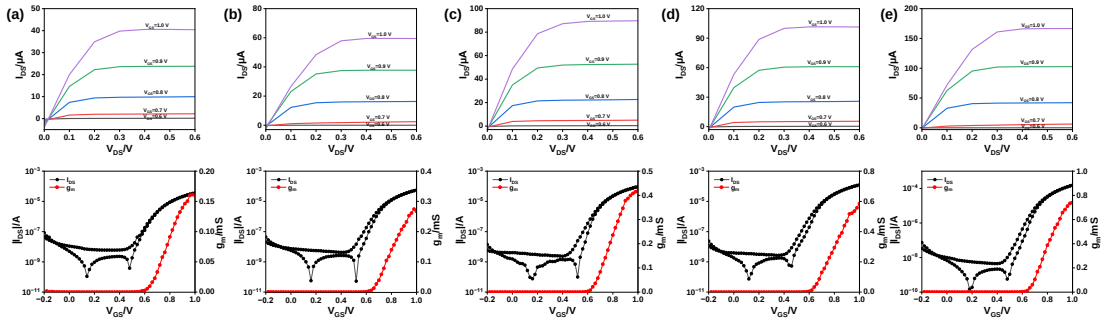

Fig. S1. Output and transfer curves of devices with different channel L/W parameters. a) 10 μm/100 μm, b) 10 μm/200 μm, c) 10 μm/ 300 μm, d) 10 μm / 400 μm, e) 10μm/500μm.

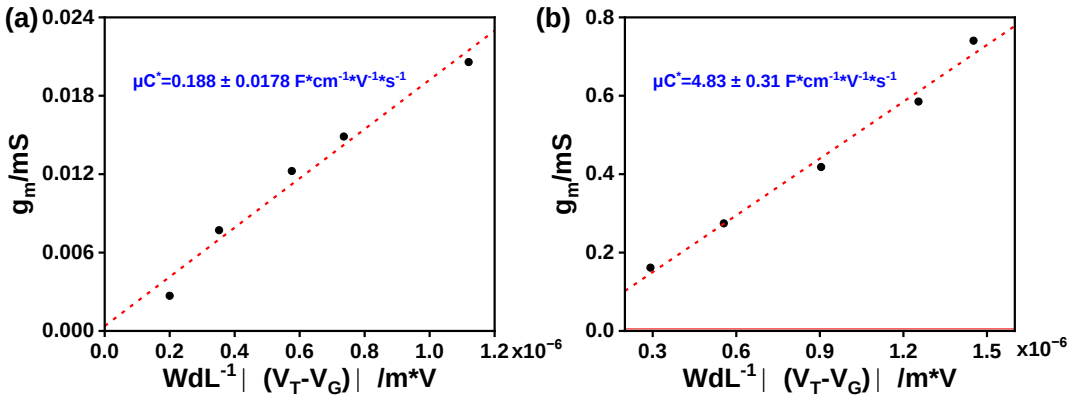

Fig. S2. The calculated μC^* before a) and after annealing b). The μC^* is extracted according to the equation $g_m = \frac{Wd}{L} \times \mu_{OECT} \times C^* \times |V_T - V_G|$, where W and L are the width and length of the channel, respectively, d is the film thickness, μ_{OECT} is the charge carrier mobility, C* is the volumetric capacitance, V_G is the gate voltage, and V_T is the threshold voltage.

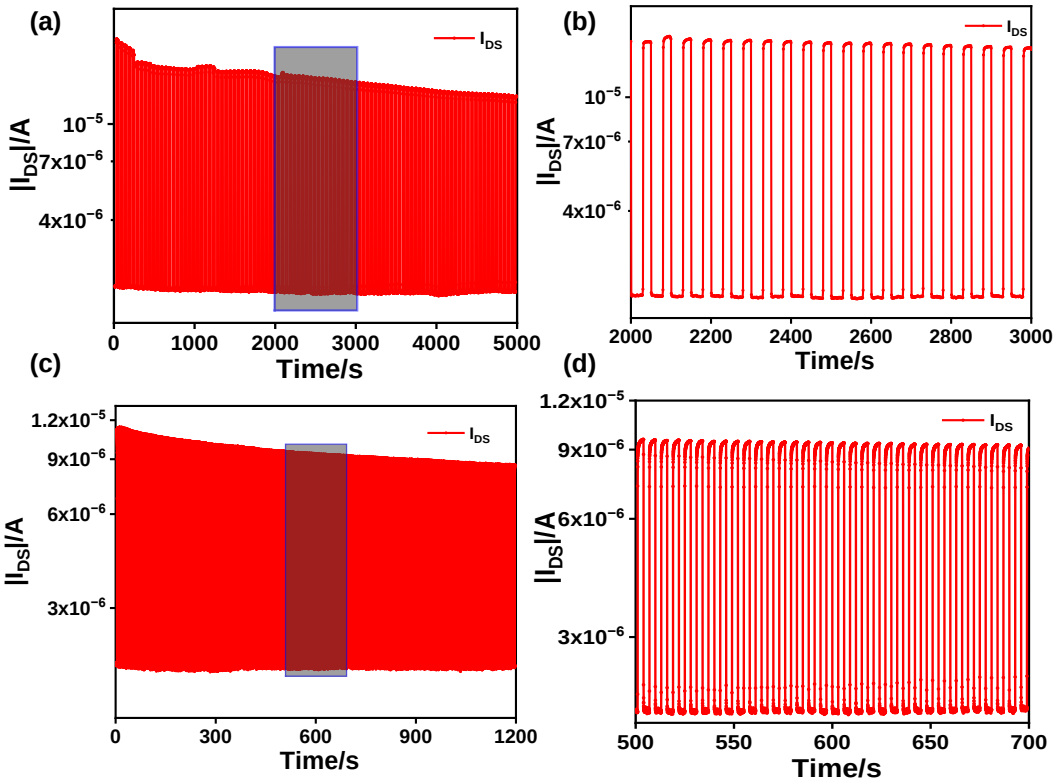

Fig. S3. (a-b) I-t of 100 cycles with each cycle lasting for 50 seconds and an enlarged view of 20 cycles, indicated by the blue box in (a). (c-d) I-t of 200 cycles with each cycle lasting for 6 seconds and an enlarged view of 33 cycles, indicated by the blue box in (c). During these cycles, V_{GS} switches between 0.6 V and 1.0 V, V_{DS} is 0.6 V.

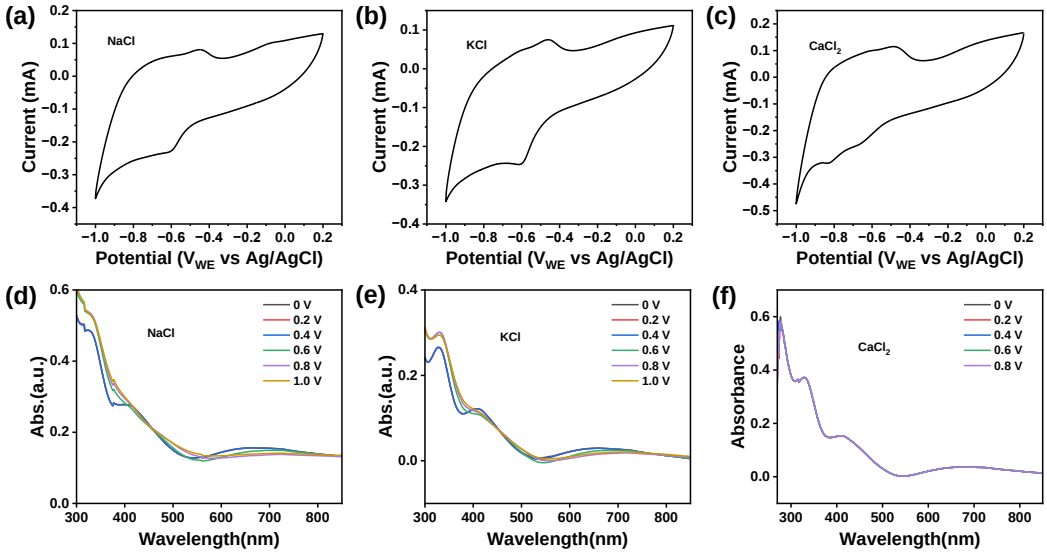

Fig. S4. (a-c) Cyclic voltammetry of $PrC_{60}MA$ thin films in different electrolytes (0.1 mol/L NaCl, KCl, $CaCl_2$) at 50 mV/sec, showing the n-doped current. (d-f) UV-Vis-NIR absorption spectrum of the $PrC_{60}MA$ film. For all measurements the voltage is applied vs an Ag/AgCl electrode with steps of 0.2 V.

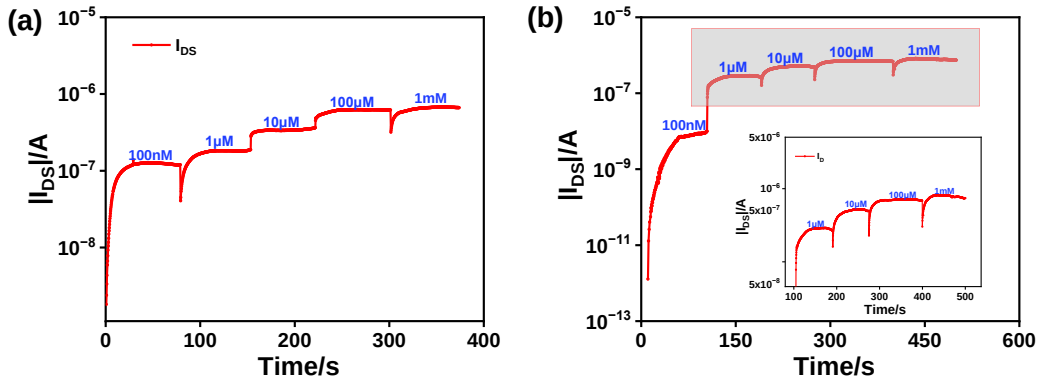

Fig. S5. The device responds to a) Na^+ and b) K^+ concentrations ranging from 100 nM to 100 μM.

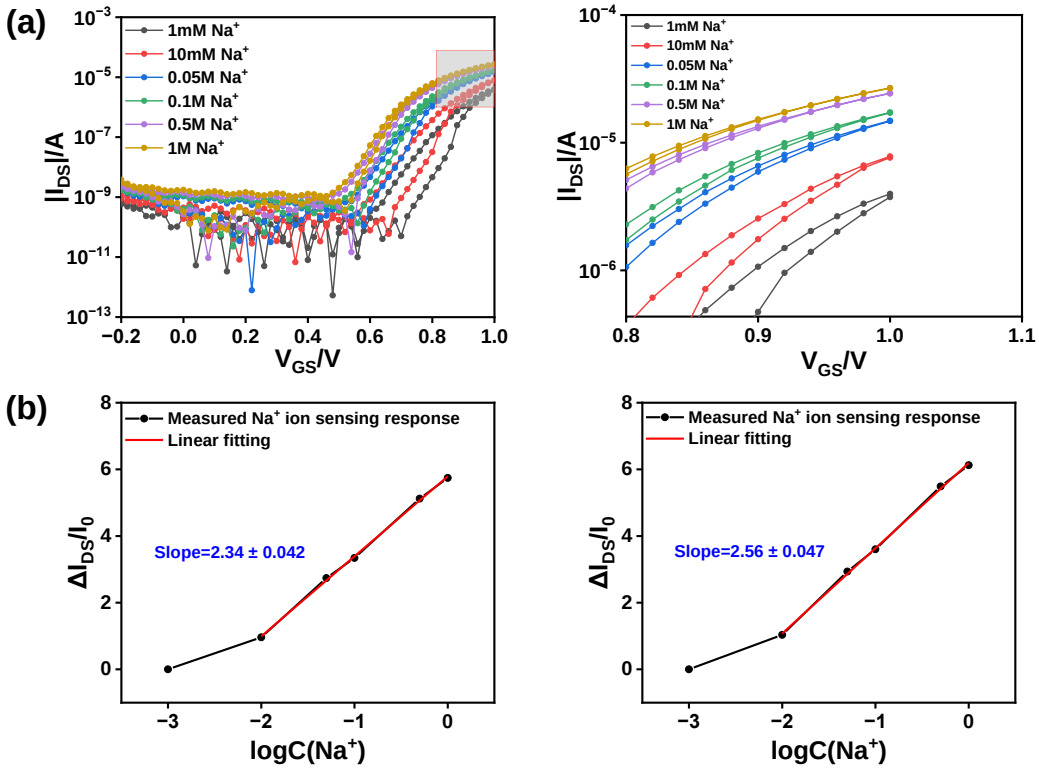

Fig. S6. (a) The transfer curve of the device to with electrolyte concentration from 1 mM to 1 M of Na^+ and its amplification diagram. (b) Normalized fitting of transfer curve current obtained by different groups of parallel experiments.

Table. S1. Comparison of ion sensors based on OECT, including ion type, limit of detection (LOD), sensitivity and linear range, etc. For more performance comparisons related to ion sensors, please refer to our previous review article (doi: 10.1002/adma.202308952).

Device	OSC materials	Analyte	LOD	Sensitivity	Linear range	Ref.
OECT	PEDOT:PSS	Na^+	/	0.35/dec	100 μM - 1 M	1
OECT	PEDOT:PSS	Na^+, K^+	/	0.71/dec (Na^+) 3.49/dec (K^+)	10 mM - 1 M	2
OECT	PEDOT:PSS MWCNT	K^+	1 nM	0.35/dec (K^+)	5 nM - 1 μM	3
OECT	PEDOT:PSS	K^+	10 μM	/	/	4
OECT	PEDOT:PSS [MTEOA][MeOSO3]	Na^+, K^+	0.75 mM (Na^+) 0.80 mM (K^+)	312 μA/dec (Na^+) 488 μA/dec (K^+)	1 mM - 0.1 M	5
OECT	p(T15c5-ran-EDOT)	Na^+	20 μM	37 μA/dec	10 μM – 1 M	6
OECT	p(T18c6-ran-EDOT)	K^+	0.1 mM	49 μA/dec	0.1 mM – 1 M	6
OECT	PEDOT:PSS BBL	K^+	/	995 mV/dec (K^+)	10 μM – 1 M	7
OECT	$PrC_{60}MA$	Na^+ K^+ Ca^{2+}	100 nM 100 nM 25.5 μM	17.35 ± 0.98/dec(Na^+) 7.21 ± 0.12/dec(K^+) 4.62 ± 0.18/dec(Ca^{2+})	10 mM - 1 M 5 mM - 1 M 255 μM - 0.255 M	This work

1. Kim, Y.; Lim, T.; Kim, C.-H.; Yeo, C. S.; Seo, K.; Kim, S.-M.; Kim, J.; Park, S. Y.; Ju, S.; Yoon, M.-H., Organic electrochemical transistor-based channel dimension-independent single-strand wearable sweat sensors. *NPG Asia Materials* **2018,** *10* (11), 1086-1095.

2. Coppedè, N.; Giannetto, M.; Villani, M.; Lucchini, V.; Battista, E.; Careri, M.; Zappettini, A., Ion selective textile organic electrochemical transistor for wearable sweat monitoring. *Organic*

Electronics **2020,** *78*, 105579.
3. Wang, Y.; Wang, Y.; Zhu, R.; Tao, Y.; Chen, Y.; Liu, Q.; Liu, X.; Wang, D., Woven fiber organic electrochemical transistors based on multiwalled carbon nanotube functionalized PEDOT nanowires for nondestructive detection of potassium ions. *Materials Science and Engineering: B* **2022,** *278*, 115657.
4. Wang, N.; Liu, Y.; Fu, Y.; Yan, F., AC Measurements Using Organic Electrochemical Transistors for Accurate Sensing. *ACS Appl Mater Interfaces* **2018,** *10* (31), 25834-25840.
5. Li, T.; Cheryl Koh, J. Y.; Moudgil, A.; Cao, H.; Wu, X.; Chen, S.; Hou, K.; Surendran, A.; Stephen, M.; Tang, C.; Wang, C.; Wang, Q. J.; Tay, C. Y.; Leong, W. L., Biocompatible Ionic Liquids in High-Performing Organic Electrochemical Transistors for Ion Detection and Electrophysiological Monitoring. *ACS Nano* **2022,** *16* (8), 12049-12060.
6. Wustoni, S.; Combe, C.; Ohayon, D.; Akhtar, M. H.; McCulloch, I.; Inal, S., Membrane-Free Detection of Metal Cations with an Organic Electrochemical Transistor. *Advanced Functional Materials* **2019,** *29* (44), 1-10.
7. Romele, P.; Gkoupidenis, P.; Koutsouras, D. A.; Lieberth, K.; Kovacs-Vajna, Z. M.; Blom, P. W. M.; Torricelli, F., Multiscale real time and high sensitivity ion detection with complementary organic electrochemical transistors amplifier. *Nat Commun* **2020,** *11* (1), 3743.